Applied Acoustics 224 (2024) 110162

Contents lists available at ScienceDirect

Applied Acoustics

journal homepage: www.elsevier.com/locate/apacoust

Vibration-based sound power level estimation: A method to reduce the number of sensors

Giulia Cristofori *, Emiliano Mucchi

University of Ferrara, Engineering Dept., Via G. Saragat, 1 - 44122, Ferrara, Italy

ARTICLE INFO

Keywords:
Radiation efficiency
Sound power
Accelerometers

ABSTRACT

The acoustic description of an industrial machine is crucial as it can provide information about its health status and assess the effectiveness of design modifications. Experimental acoustical measurements exist, but they may be impractical in noisy environments and limited by spatial requirements. Vibration-based approaches have been explored to overcome these limitations. However, the experimental procedure requires a large number of sensors. The aim of this work is to introduce a novel method which, starting from the vibration-based procedure, allows to reduce the number of sensors required to accurately estimate the sound power. An analysis of the number and the position of the accelerometers has been conducted to find the positions that better fit the resulting vibration-based sound power. An experimental campaign on a system consisting of a worm gear gearbox driven by an electrical motor has been used as a case study to verify the accuracy of the procedure. Acoustical based measurements were conducted and used as reference. Thus, starting from the data of twenty-seven accelerometers, the improved procedure was performed. The results will be plotted considering two and four accelerometers as input data and four operational conditions. The resulting vibration-based sound power levels demonstrate a good agreement in both octave bands and overall values.

Furthermore, the trend of the radiation factor was investigated, aiming to determine the influence of parameters such as resistant torque and rotational velocity.

1. Introduction

The characterization of industrial machinery through acoustics is of growing interest in the mechanical field, as it allows information about the state of health of a component or comparison between different design configurations. As a consequence, the definition of a reliable procedure to easily derive the acoustical magnitudes is an interesting topic. Within this contest, radiated sound power is a quantity that allows a deep characterization of a mechanical component in terms of acoustical emission. Differing from the acoustical pressure and the acoustical intensity, the acoustical power does not depend on the distance between the measurement location and the source but it is a property of the sound source. Nevertheless, the measurement techniques may be troublesome, especially considering industrial environments affected by predominant background noises and impractical test benches.

Currently, the experimental procedures for evaluating acoustic sound power are based on acoustical measurements. Standard ISO 3741 and 3743, based on the measure of the sound pressure, may be employed in reverberating test rooms, while Standard ISO 3744, 3745 and 3746 [1] may be employed in free fields. As an alternative, starting from the knowledge of the acoustic intensity, the standard ISO 9614 [2] has no limitations on the type of acoustic field but can be troublesome regarding the spatial requirements.

This work aims to find methodologies more accessible for acoustic power determination, based on the acceleration signal processing since the accelerometers have low spacial requirements and are not affected by background noises. Since the goal is to investigate the link between the radiated power and the vibration of the structure, it has been essential to introduce a dimensionless quantity called radiation resistance (or radiation efficiency, or radiation factor) described in Eq. (1). As suggested by Fahy and Brancati [3], the radiation resistance is defined as the ratio between the averaged radiated sound power ($\overline{W}$) and the sound power radiated in the far-field by a circular rigid piston with surface S and vibrating with mean-square-velocity $\overline{v^2}$:

$$\sigma = \frac{\overline{W}}{\rho_0 c S \overline{v^2}} \tag{1}$$

* Corresponding author.
E-mail address: crsgli1@unife.it (G. Cristofori).

https://doi.org/10.1016/j.apacoust.2024.110162
Received 4 April 2024; Received in revised form 1 July 2024; Accepted 3 July 2024
Available online 11 July 2024

Nomenclature

Greek Symbols

Δ	Difference between acoustical-based and vibration-based sound power levels
Γ	Index indicating the spectral similarity
ρ	Air density
σ	Radiation resistance

Latin Symbols

a	Acceleration signal
c	Velocity of sound in air
k	Combination of accelerometer
k'	First reduced combination of accelerometers
k''	Final improved combination of accelerometers
m	Number of operational conditions
n	Number of reduced accelerometers
N_t	Number of considered operational conditions
p	Number of starting accelerometers in the improved procedure
S	Vibrating surface
v	Vibrating velocity signal
W	Radiated sound power
Z_c	Characteristic impedance of air

Subscripts

0	Subscript indicating the reference value
ac	subscript representing the acoustical-based quantities
i	subscript representing the accelerometer position
j	subscript representing the octave frequency band
vib	subscript representing the vibration-based quantities

ρ_0 is the mean air density (kg/m^2) and c the velocity of sound in air (m/s). It must be noted that the theoretical circular rigid piston has to be large with respect to the wavelength of the airborne sound. The radiation resistance depends on the geometry, the thickness of the radiating object, the excitation source [4], the boundary conditions [5] and the modal pattern [6].

A literature review has demonstrated the existence of analytical procedures to define the radiation factor and the radiated power, nevertheless, they were limited to simple geometries. Finite rectangular panels with different boundaries ([7],[8],[9],[10]) and annular guided plate [11] have been investigated. The outstanding methodologies to determine the sound power are the Rayleigh Integral Method (RIM) [12], the Discrete Calculation Method (DCM) [4], the Integral Transform Method (ITM) [13] and the modal summation approach (MS) [6]. Conta et al. [14] described and compared the RIM, the DCM and the ITM methodologies on planar objects with impact excitations. A description of the radiation efficiency of cross-laminated plates has been done by Santoni et al. [15], investigating the influence of the number of measurement points and their distribution on the surface. They concluded that, as long as the number of considered positions is fairly high, the local position of each single transducer plays a less important role.

Since applying the analytical methodologies may be impractical for complex geometries, alternative experimental and numerical procedures have been investigated. Jacobson et al. [16] experimentally defined the radiation factor of a gearbox using only three accelerometers and sound intensity measurements as input data. Hence, the gearbox faces have been simplified as vibrating flat panels and the radiation efficiency has been computed with ideal acoustical models. They have found that the analytical results do not adequately simulate the experimental radiation behavior of the gearbox. Revel and Rossi [17] derived the sound power level of a loudspeaker diaphragm with numerical simulations, analytical procedures, acoustic intensity techniques and the Standard ISO 7849 based on the experimental vibration data acquired with a laser Doppler. The last procedure has been found to be the fastest and easiest to implement with a good accuracy of the results, nevertheless, the loudspeaker is still a simple and planar geometry. Yantek [18] employed the vibration methodology to investigate the influence of different modifications on a continuous miner tail section considering a unitary radiation factor. The results, in terms of modification efficacy, show good accuracy in comparing the vibration sound power level and the acoustic pressures. Nevertheless, the radiation efficiency behavior has not been investigated. Abouel-Seoud et al. [19] predict the radiation factor of a gearbox, employing the RIM and considering the gearbox surfaces as a set of flat panels. Nevertheless, no verification has been conducted on the accuracy of the results considering a radiation efficiency experimentally assessed. Barelli et al. [20] compared the vibration-based methodology with the acoustical intensity measurements on a cogenerative internal combustion engine, subdividing the external surfaces into three areas that show different frequency trends of the radiation factor: although, they have not done a sensitive analysis on the number of accelerometers and several differences have been found in the resulted radiation efficiency of the three considered areas. An alternative approach to measuring the vibration velocities has been proposed by Gardonio et al. [21] that found the sound radiation of a baffled rectangular panel starting from the vibratory velocity acquired with a set of six cameras. The sound radiation into free-field has then been estimated by using the RIM. Nascimento et al. [22] compared the sound power level of refrigeration compressors with two methodologies based on acceleration data analysis: ISO 7849 and a data-driven soft sensor method.

This work aims to employ a vibration-based procedure to measure the radiated sound power of a machine with experimental accelerations as input data, allowing to overcome the limits related to the existing methodologies. For real, the acoustical experimental measurements are limited by the background noises and spatial requirements. The originality of the work regards the developed novel methodology to reduce the number of accelerometers from the quantity proposed by the Standard ISO 7849-2 maintaining the accuracy of the results. Once the methodology is developed and verified, the reduced number of accelerometers can be used to compare different prototypes in the R&D phase within time and cost limitations. It can also be used for end-of-line testing, making the procedure easy and repeatable.

The procedure to define the radiation factor from the experimental vibration data has been described in Sec. 2. Hence, in Sec. 3, the methodology has been described to find the best localization of a reduced number of sensors. In Sec. 4 the experimental campaign has been described. The results of the improved procedure were presented and discussed in Sec. 5. Sec. 6 provides a detailed analysis of the radiation factor in various operating conditions. Finally, Sec. 7 summarizes the obtained results.

2. Overview of the vibration-based procedure

The procedure to evaluate the vibration-based sound power and the radiation efficiency of a complex geometry has been assessed following ISO-TS 7849-2 [23]. The first step consists of discretizing the radiating surfaces into smaller areas. The standard helps in defining the correct number of sensors. The flowchart in Fig. 1 describes the step of the procedure: initially, a first-attempt finite number i of accelerometers must be chosen following the suggestion in the Standard ISO-TS 7849-2. The number of accelerometers will be adjusted as described hereinafter.

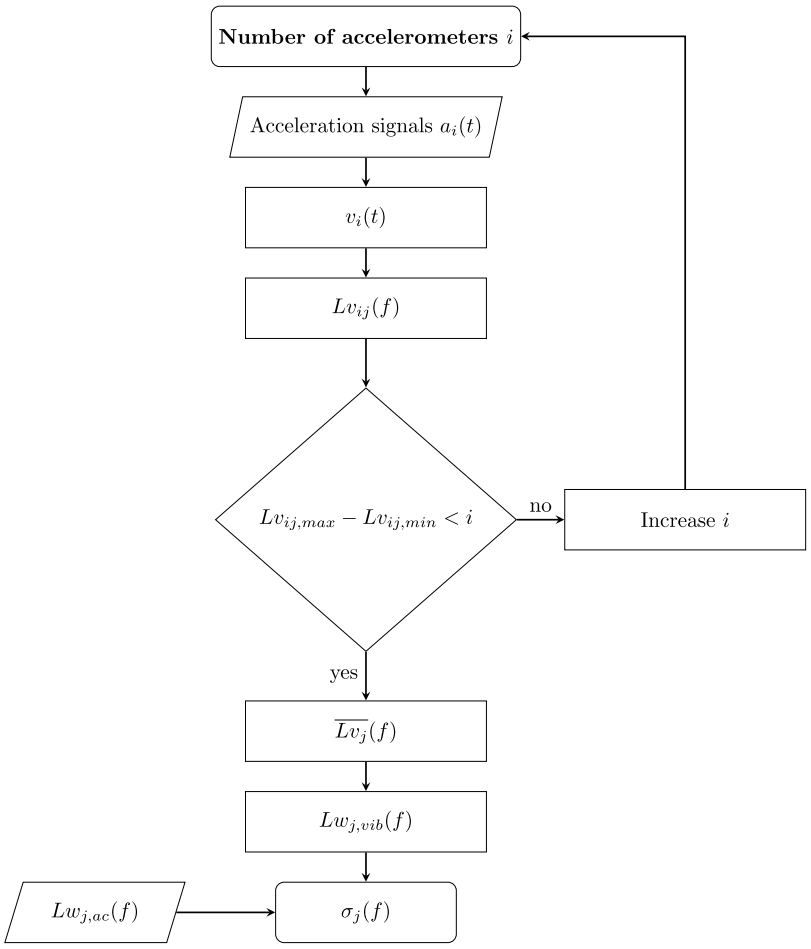

Fig. 1. Flowchart for the radiation factor evaluation starting from the vibration-based data.

For each measurement point i, the RMS value of the acceleration normal to the surface (a_i) is acquired and, consequently, integrated to obtain the RMS value of the vibratory velocity (v_i). Then, from the velocity spectra, the velocity levels (Lv_{ij}) are assessed, in one-third octave bands, for each accelerometer:

$$Lv_{ij} = 10\log_{10}\frac{v_{ij}^2}{v_0^2}\ \text{dB} \tag{2}$$

where $v_0 = 5x10^{-8} m/s$ is the velocity reference value.

Following standard ISO 7849-2, the number of measurement points must be increased if the difference between the maximum and the minimum value of the vibratory velocity level exceeds the number of chosen accelerometers, considering each one-third octave band. Once a proper number of sensors is identified, the surface averaged velocity level is derived with the following equation:

$$\overline{L}v_{ij} = 10\log\left(\frac{1}{S}\sum_{i=1}^{N} S_i 10^{0.1Lv_{ij}}\right)\ \text{dB} \tag{3}$$

where S is the total radiating area and S_i is the partial area associated with measurement point i. Finally, the vibration-based radiating power is computed, considering a unitary radiation efficiency:

$$Lw_{j,vib} = \overline{L}_{v,j} + 10\log_{10}\frac{S}{S_0}\ \text{dB} + 10\log_{10}\frac{Z_c}{Z_{c,0}}\ \text{dB} \tag{4}$$

where $Z_{c,0}$ is the reference value of the which value is 411 Ns/m^3 and S_0 is the surface reference value of 1 m^2. Eventually, the radiation factor is computed as the ratio between the acoustical-based sound power and the vibration-based sound power:

$$\sigma_j = \frac{W_{ac,j}}{W_{vib,j}} \tag{5}$$

3. Novel approach to reduce the number of sensors

It should be noted that the major limitation of the aforementioned procedure is related to the number of sensors required, since an experimental setup with several accelerometers can be impractical and expensive, especially in industrial environments. This consideration leads us to look for an alternative test setup with fewer measurement points with a reasonable accuracy of the results in terms of emitted sound power.

The flowchart in Fig. 2 describes the procedure to find which are the better accelerometer positions given a fixed number of sensors, with reference to an initial setup of several sensors. The initial sensor data recommended by the Standard is essential for the proposed methodology as it enables the identification of the optimal accelerometer positions. Thus, starting from these data, the reduced number of sensors found with the proposed procedure may be useful for comparing similar prototypes in the research and development phase and for end-of-line verifications.

The starting setup consists of a number p of accelerometers, chosen following the Standard ISO 7849-2: for each sensor, the RMS value of the acceleration normal to the radiating surfaces has been acquired. The first step of the procedure consists of choosing the number of reduced accelerometers (n) and the number of operational conditions to optimize (m). Thus, following the signal processing described in the previous sections, the overall vibration-based sound power level has been computed for all the combinations of accelerometers considered, namely k_m. The number of combinations is described in Eq. (6).

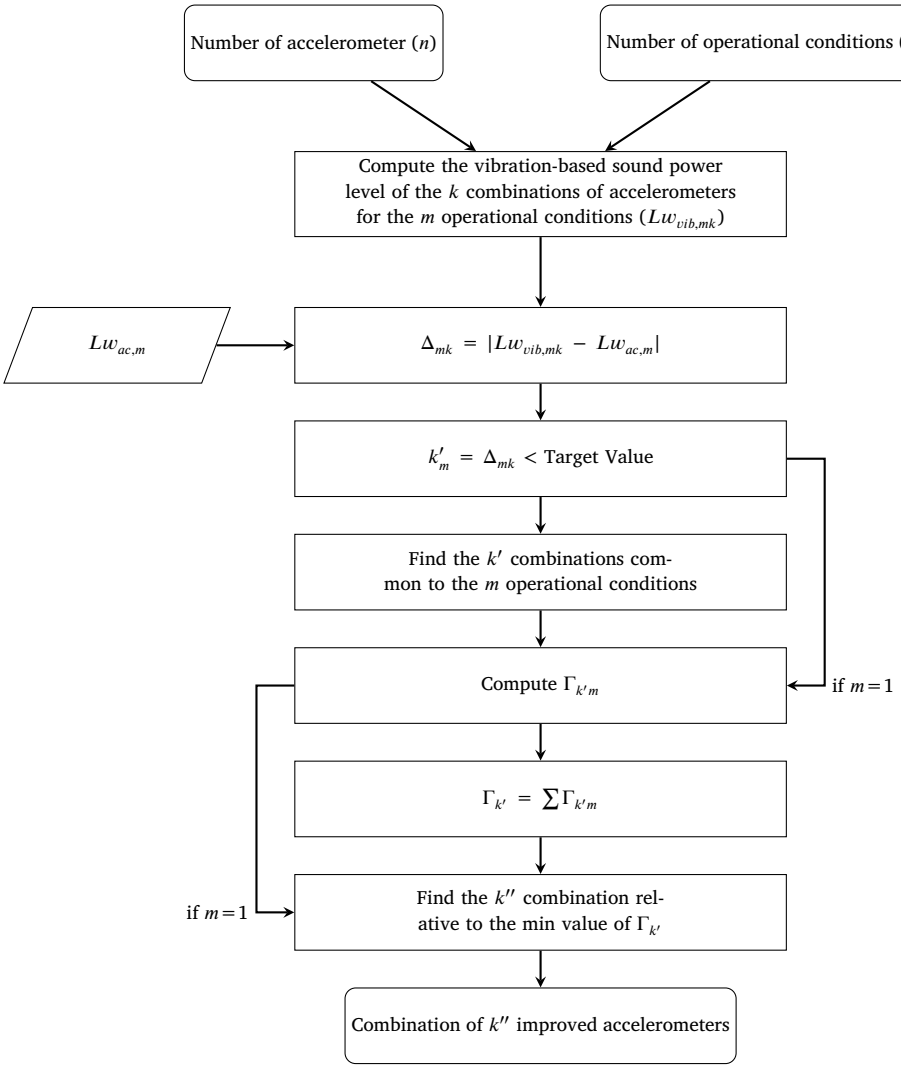

Fig. 2. Flowchart of the procedure to optimize the position of the accelerometers.

$$k_m = p^n \tag{6}$$

It is worth noting that, considering a reduced number of sensors, the measurement surfaces were equally subdivided between the selected measurement points to enhance the efficacy of the procedure. Thus, Eq. (3) changes as follows:

$$\overline{Lv}_{ij} = 10\log\left(\frac{1}{n}\sum_{i=1}^{n} 10^{0.1Lv_{ij}}\right) \text{ dB} \tag{7}$$

A first cut of the combinations of accelerometers is made, keeping the k'_m combinations of accelerometers for which the absolute value of the difference between the acoustical-based and vibration-based overall sound power levels (Δ_{mk}) is less than a given Target Value. Therefore, the number of combinations is still reduced at k' combinations considering which of the k'_m combinations is common at each considered operational condition.

Since considering only the overall values may be misleading, the octave band sound power levels are investigated in order to deepen the resemblance between acoustical-based and the vibration-based data. As a consequence, an index namely Γ is proposed to quantify, with a numerical value, the similarity between different frequency spectra, giving more weight to the frequency band with higher values:

$$\Gamma_{k'} = \frac{\sum_j \sqrt{\Delta_{j,k'} Lw_{j,ac}}}{\sum_j Lw_{j,ac,k'}} \tag{8}$$

where $\Delta_{j,k'}$ is the difference between the acoustical-based and the vibration-based sound power levels, for each j-th frequency band. It is worth noting that the vibration-based sound power levels were computed from the k' combinations of accelerometers.

Finally, to combine the Γ_m values of each test, a sum of the indexes of each considered operational condition has been done and the resulting minimum value has been employed to define which of the combinations studied give the best results in terms of sound power level with reference to the acoustical-based values. The output of the procedure is the k'' combination of n accelerometers that optimizes the position of the accelerometers, for m operational conditions, simultaneously.

4. Experimental assessment

An experimental campaign has been conducted to verify the proposed methodology. The system under examination consists of a worm gear mechanism driven by an electrical engine. The test bench allows the control of the worm velocity at the input shaft and the resistant torque on the gear at the output shaft (Fig. 3). Therefore, different operational conditions, described in Table 1, were tested. Tests 1 to 4 employ a constant power supply frequency across a range of torque values, whereas tests 5 to 8 utilize a variable power supply frequency without a resistant torque on the gear. The operational conditions were selected to investigate the influence of torque and velocity on the resulting sound power levels. Furthermore, it is noteworthy that the zero-torque condition was

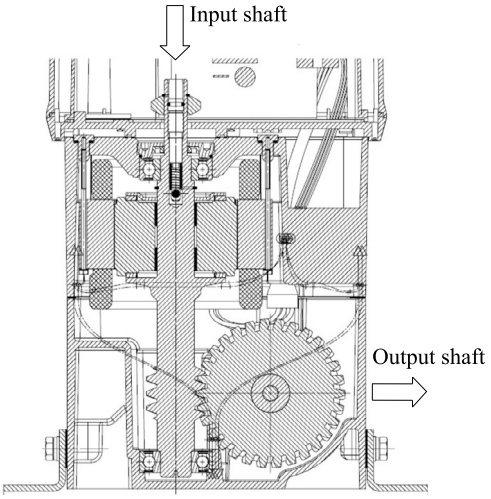

Fig. 3. Scheme of the system under study.

Table 1
Details of the experimental tests conducted.

	Power supply frequency	Resistant torque on the gear
Test 1	70 Hz	4 Nm
Test 2	70 Hz	8 Nm
Test 3	70 Hz	12 Nm
Test 4	70 Hz	18 Nm
Test 5	40 Hz	0 Nm
Test 6	60 Hz	0 Nm
Test 7	70 Hz	0 Nm
Test 8	80 Hz	0 Nm

chosen as it represents a typical operational scenario in which the torque is relatively low.

Both the vibration-based and the acoustical-based measurements were conducted for each test. The acoustical-based measurements were used as reference data to analyze the differences between the sound power levels obtained from the two methods.

4.1. Acoustical measurements

The evaluation of the acoustical sound power level emitted by the system has been carried out according to the standard ISO 3746 [1]. This standard was chosen due to limitations on the measurement location. The reference box, enclosing the noise source, has a size of 14 cm x 19.5 cm x 23 cm. The measurement surface, representing the surface on which the microphones are placed for the sensing of the sound pressure, were defined at a distance of 30 cm from the reference box. In particular, eight microphones have been placed around the system. Fig. 4 summarizes the sensor positions: four microphones in the upper vertexes, one in the middle of the upper face and three in the middle of three vertical faces, excluding the one where the connection to the electric engine hinders the positioning of a microphone.

4.2. Vibration measurements

The number of accelerometers selected adheres to Standard ISO 7849-2, which mandates that the difference between the maximum and minimum velocity levels must be less than the number of sensors in each one-third frequency band. The Standard recommends using ten sensors for this measurement surface. However, the resulting vibratory velocity levels do not meet the verification requirements of the standard with this number of accelerometers. Thus, the procedure was repeated increasing the number of sensors at fifteen, twenty and finally twenty-seven. A monoaxial accelerometer has been mounted on each of these surfaces

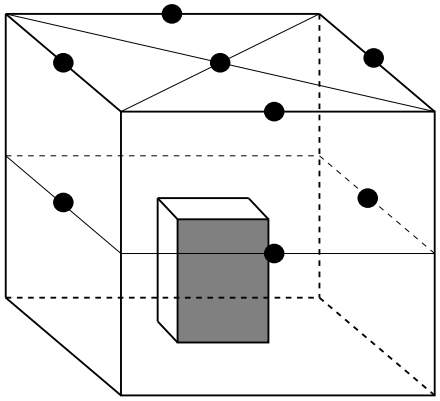

Fig. 4. Scheme of the positions of the microphones during the acoustical measurements.

(model PCB 356B2, sampling frequency 25600 Hz and 1 Hz resolution) since the interest is to measure the RMS value of the vibratory velocity normal to the radiating surface. The results obtained with less than twenty-seven accelerometers were not presented for the sake of brevity since they not meet the verification requirements. Fig. 5a shows the vibratory velocity levels for each one-third octave frequency band and each accelerometer. Fig. 5b shows, for each one-third octave band, the difference between the maximum and the minimum vibratory velocity level and the red line represents the number of employed accelerometers. Fig. 5 shows the data acquired during Test 1, analogous results were obtained for the other tested operational conditions, even though they are not plotted for the sake of brevity. The location of the accelerometers is shown in Fig. 6. Each point of measure is related to a representative surface and the total radiating area is 0.1635 m^2.

5. Application and assessment in a real case scenario

As a first attempt, the optimization of the existing twenty-seven sensors, shown in Fig. 6, has been performed considering two accelerometers and one operational condition. Thus, four operational conditions were optimized simultaneously: with a constant rotational velocity and different torques. Finally, the sound power levels have been computed considering four accelerometers to investigate how the output varies with an increased number of sensors. It is worth noting that the sound power levels will be presented in octave bands, as ISO 3746 permits obtaining the acoustical-based sound power level in octave bands. For the sake of brevity, the proposed procedure was implemented on Tests from 1 to 4. The other tests give analogous results.

5.1. Optimization with two accelerometers - one operational condition

Before starting with the signal processing, the number k of combinations has been reduced by removing the redundant couples passing from 729 combinations, defined by Eq. (6), to 351. For each of these combinations, the vibration-based sound power levels have been computed following the procedure in Sec. 2 and considering the acceleration data as input. The absolute values of the difference between the overall vibration-based and acoustical-based sound power levels were investigated and described in Fig. 7, which summarizes the data for each combination of accelerometers. Table 2 lists the number of combinations of accelerometers for which the difference between the acoustical-based and the vibration-based sound power levels is lower than the Target Value, set as 1 dB(A). Test 1 has the lowest number of k'_m, while Test 4 has the highest number of k'_m.

After improving each test individually, the resulting sound power levels are displayed in Fig. 8, revealing intriguing findings. First, it is interesting to note that the improved accelerometers varied for the tested operational conditions. The couple of accelerometers (10,14) optimizes

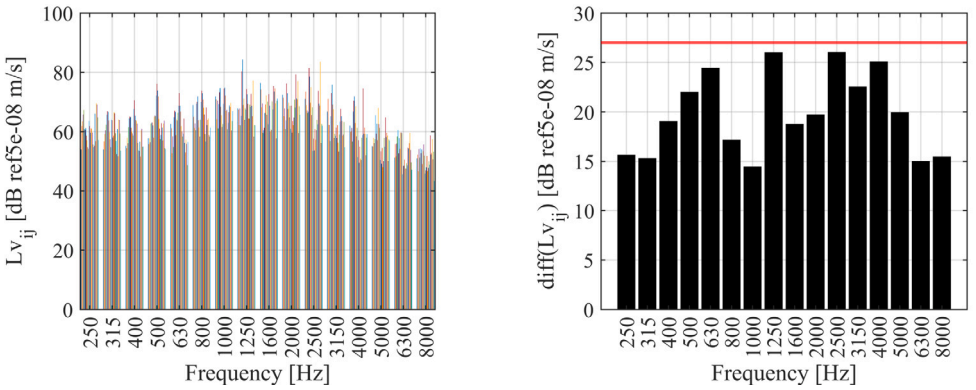

(a) Vibratory velocity levels for each one-third octave frequency band and each accelerometer

(b) Differences between the vibratory velocity levels within different accelerometers

Fig. 5. Velocity levels of Test 1

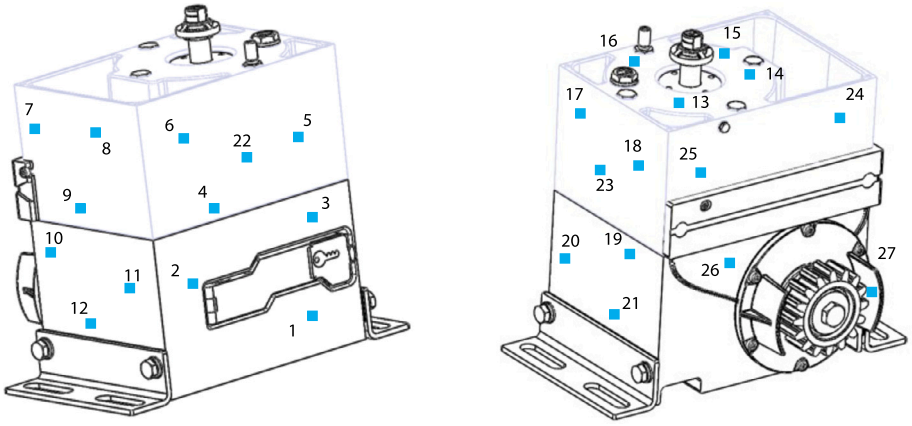

Fig. 6. Position of the accelerometers in the experimental setup.

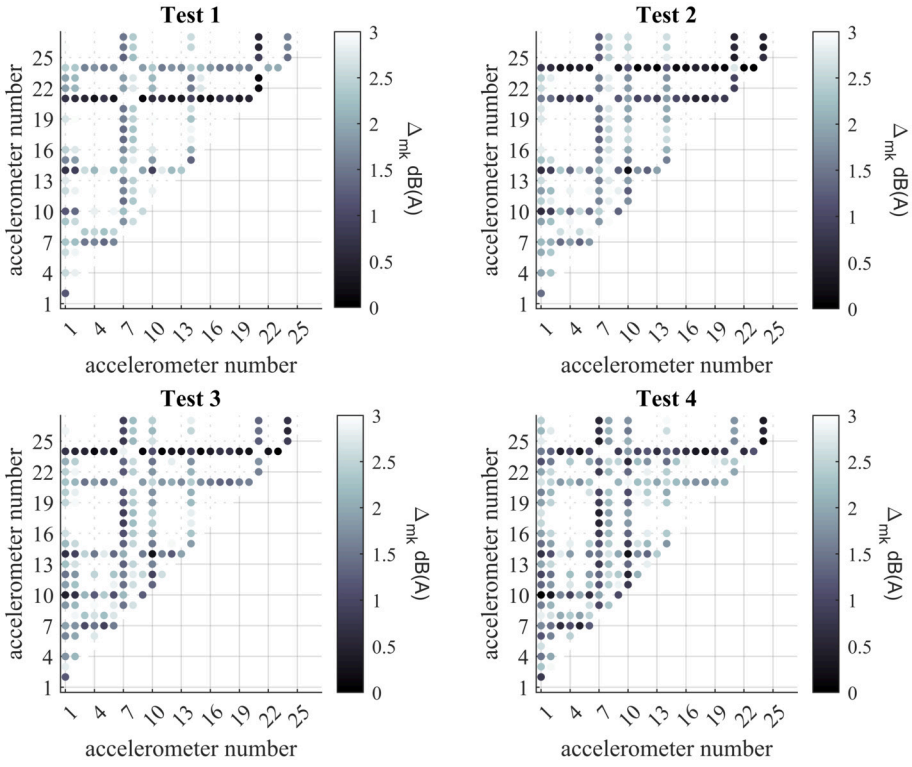

Fig. 7. Absolute values of the differences between the overall vibration-based sound power level and the acoustical-based sound power level.

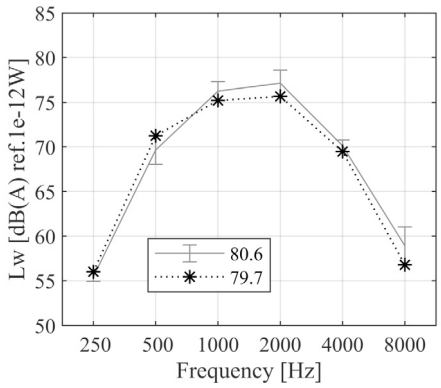

(a) Test 1. Vibration-based data computed from the data of the k" optimized accelerometers (10,14)

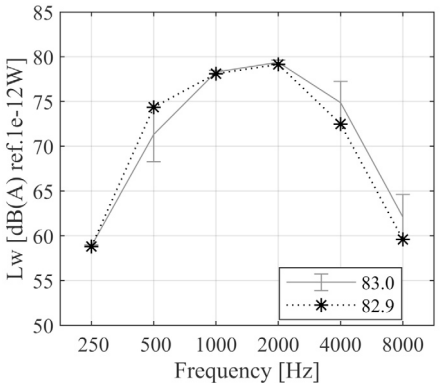

(b) Test 2. Vibration-based data computed from the data of the k" optimized accelerometers (10,14)

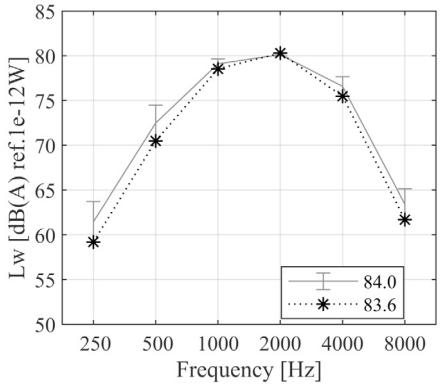

(c) Test 3. Vibration-based data computed from the data of the k" optimized accelerometers (1,10)

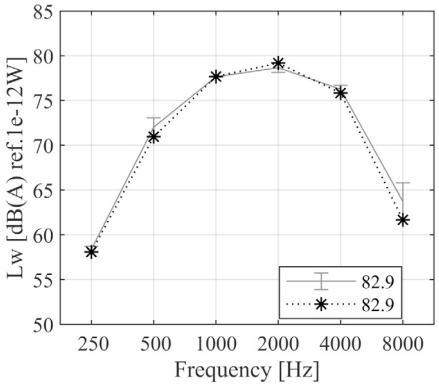

(d) Test 4. Vibration-based data computed from the data of the k" optimized accelerometers (1,10)

Fig. 8. Acoustical-based sound power level (-) and vibration-based sound power level (:*) computed from the data of the k'' optimized accelerometers. Overall and octave bands results.

Table 2
Number of combinations of two accelerometers for which the difference between the overall acoustical-based and vibration-based sound power level is lower than the Target Value.

	Test 1	Test 2	Test 3	Test 4
k'_m	40	65	62	68

Table 3
Improved procedure results considering two accelerometers and one operational condition. Comparison concerning the overall sound power levels.

	Test 1	Test 2	Test 3	Test 4
k''	(10,14)	(10,14)	(1,10)	(1,10)
Lw_{ac} [dB(A)]	80.6	83.0	84.0	82.9
Lw_{vib} [dB(A)]	79.7	82.9	83.6	82.9
Δ_{mk} [dB(A)]	0.9	0.1	0.4	0
$\Delta\%_{mk}$ [%]	1.12	0.12	0.48	0

Test 1 and Test 2, while the couple (1,10) optimizes Test 3 and Test 4. The obtained overall sound power levels were summarized in Table 3, which contains also the differences between the acoustical-based and the vibration-based results as well as the percentage differences. The maximum percentage difference, in terms of overall sound power level, is 1.12% for Test 1 and the minimum one is 0% for Test 4.

5.2. Optimization with two accelerometers - Tests 1 to 4

As mentioned before, the proposed procedure can find an improved combination of accelerometers considering more than one operational condition. Thus, starting from the results in Fig. 7 the couples of accelerometers k' common to each of the considered four tests were individuated: the two combinations identified are the couples of accelerometers (1,14) and (10,14). Fig. 9 shows the overall sound power levels of the optimized accelerometers: the grey line represents the reference value of the acoustical-based overall sound power level and the dotted lines identify the Target Value limits.

In order to compare the frequency spectra, the Γ_m value has been computed for each combination of k' couples of accelerometers and each considered test, the results are shown in Fig. 10. Thus, the sum of the Γ_m values for each test was computed and employed to evaluate the improved couple of accelerometers. For Tests from 1 to 4, considering a number n of two sensors, the optimised position of the accelerometers was found to be the couple of accelerometers 10 with 14. This couple was the same found for the improved procedure for a single operational condition for Test 1 and Test 2. Fig. 11 shows the acoustical-based sound power level compared with the sound power level computed from the acceleration data optimized for Test 3 and Test 4. Moreover, as a confirmation of the accuracy of the procedure, the resulting overall sound power levels, whose values are listed in Table 4, have been investigated. For each test differences between the overall levels are less than the defined target value of 1 dB(A).

The differences between the acoustical-based sound power level and the vibration-based sound power level were finally investigated aiming to quantify the discrepancies and to individuate which are the critical

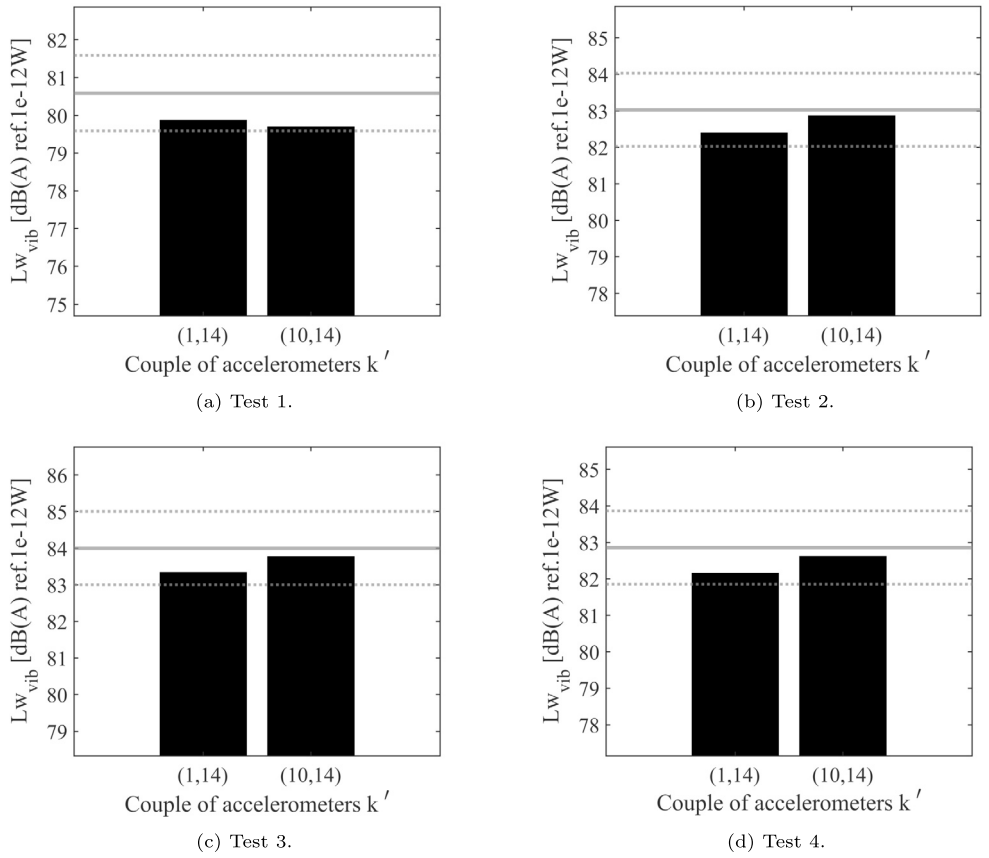

Fig. 9. Overall vibration-based sound power levels of the k' combinations of accelerometer. The gray line represents the overall acoustical-based sound power level of reference and the gray dotted lines are the difference between the overall acoustical-based sound power level and the Target Value.

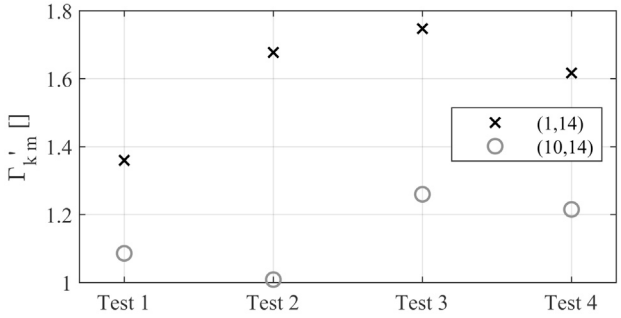

Fig. 10. $\Gamma_{k'_m}$ values for the k' combinations of the accelerometers (1,14) and (10,14).

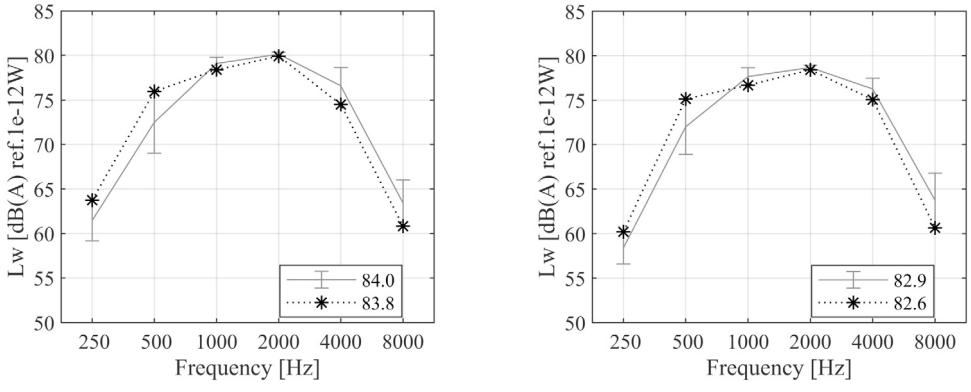

Fig. 11. Acoustical-based sound power level (-) and vibration-based sound power level (:*) computed from the data of the k'' optimized accelerometers (10,14). Overall and octave bands results.

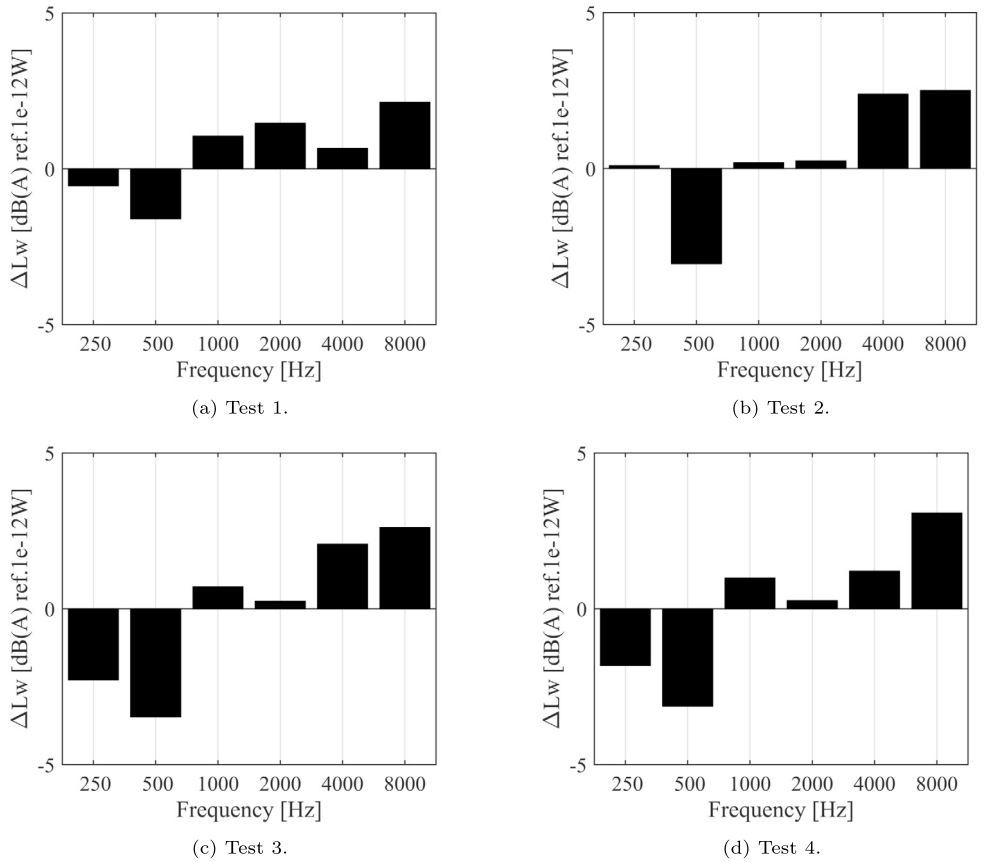

(a) Test 1. (b) Test 2.

(c) Test 3. (d) Test 4.

Fig. 12. Difference between the acoustical-based sound power level and the vibration-based sound power level.

Table 4
Improved procedure results considering two accelerometers and four operational condition. Comparison concerning the overall sound power levels.

	Test 3	Test 4
k''	(10,14)	(10,14)
Lw_{ac} [dB(A)]	84.0	82.9
Lw_{vib} [dB(A)]	83.8	82.6
Δ_{mk} [dB(A)]	0.2	0.3
$\Delta\%_{mk}$ [%]	0.24	0.36

Table 5
Number of combinations of two accelerometers for which the difference between the overall acoustical-based and vibration-based sound power level is lower than the Target Value.

	Test 5	Test 6	Test 7	Test 8
k'_m	5533	4915	5483	6080

frequency bands. Fig. 12 shows that the frequency bands that present the higher values of difference were 500 Hz and 8000 Hz. Within these frequency bands, the radiated sound power level exceeds the vibration-based sound power level of about 3 dB(A). Although, the frequency bands with the higher sound power values show a very good agreement.

5.3. Optimization with four accelerometers - Tests 1 to 4

Once the reliability of the procedure has been confirmed with a number n of two accelerometers, it has been investigated how the output data changes by adding two sensors. Tests from 1 to 4 have been investigated. Considering an initial number of four accelerometers, the number k of starting combinations has increased from 351 (with two accelerometers) to 17750. As Table 5 suggests, there were many more combinations of accelerometers for which the delta values were lower than the Target Value, with respect to Table 2.

Following the improved procedure, the resulting combination of four accelerometers that optimizes the sound power level is (2,10,14,21). For the sake of brevity, the procedure steps are not displayed. The results concerning the overall sound power levels were shown in Table 6. Fig. 13 shows the spectra results: the vibration-based sound power levels computed with the acceleration data of four improved accelerometers were in good accordance with the acoustical-based sound power levels. As a consequence, this found configuration may be suitable for four operating conditions simultaneously without any changes in the position of the accelerometers.

Table 6
Improved procedure results considering four accelerometers and four operational condition. Comparison concerning the overall sound power levels.

	Test 1	Test 2	Test 3	Test 4
k''		(2,10,14,21)		
Lw_{ac} [dB(A)]	80.6	83.0	84.0	82.9
Lw_{vib} [dB(A)]	80.1	82.8	83.8	82.8
Δ_{mk} [dB(A)]	0.5	0.2	0.2	0.1
$\Delta\%_{mk}$ [%]	0.62	0.24	0.24	0.12

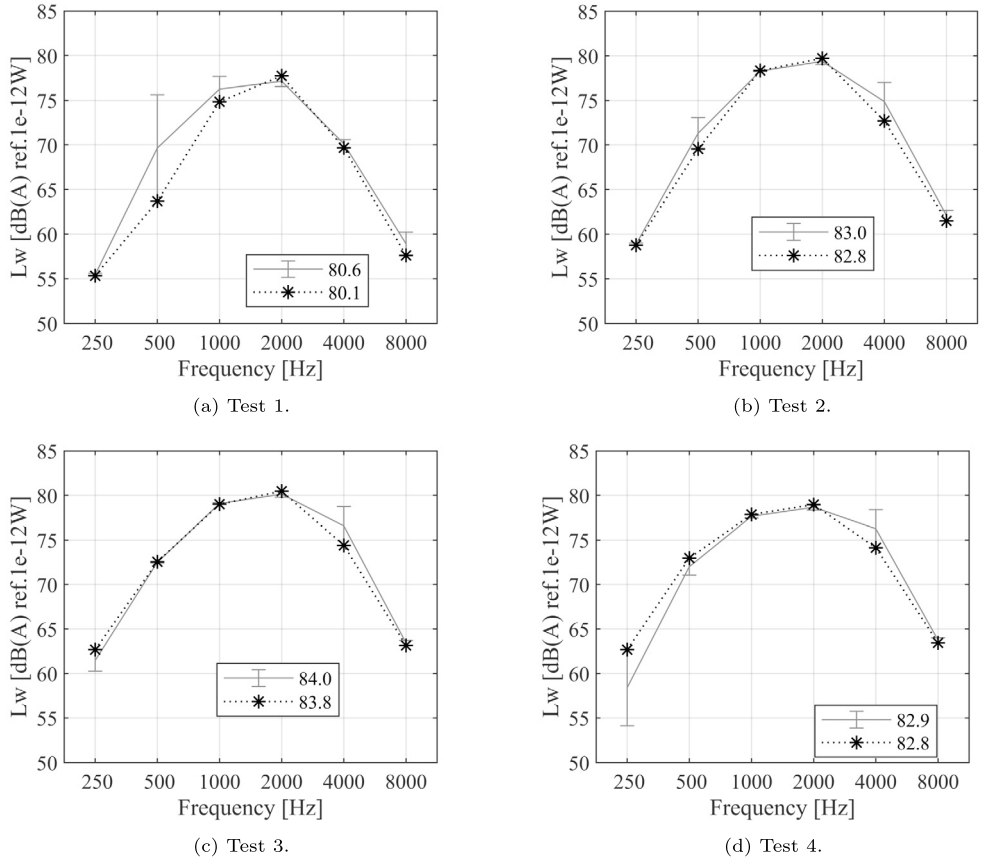

(a) Test 1. (b) Test 2. (c) Test 3. (d) Test 4.

Fig. 13. Overall vibration-based sound power levels of the k' combinations of accelerometer. The gray line represents the overall acoustical-based sound power level of reference and the gray dotted lines are the difference between the overall acoustical-based sound power level and the Target Value.

Table 7
Number of combinations (k) and computational time required depending on the number of starting accelerometers for the improved procedure (n).

Parameter	Values				
n	1	2	3	4	5
k	27	351	2925	17750	80730
Computational time (s)	9	14	62	554	21183

Table 8
Combinations of improved accelerometers depending on the different number of starting sensors.

n	Improved accelerometers k''
1	(10)
2	(10,14)
3	(2,10,14)
4	(2,10,14,21)
5	(2,6,10,14,21)

5.4. Sensibility on the number of accelerometers

The analysis of the impact of the number of chosen accelerometers on the improved procedure is crucial. The procedure has been implemented starting with a different number of sensors, ranging from one to five. A higher number of accelerometers results in longer computational time due to the rapid increase in the number of combinations to investigate, as seen in Table 7. Table 8 lists the combinations of accelerometers resulting from the improved procedure for the sensor positions shown in Fig. 6. It is worth noting that, by increasing the number of accelerometers in the improved procedure, the positions of the resulting accelerometers remain unchanged. For instance, accelerometer 10 is present in all obtained combinations.

The investigation began with the analysis of the overall sound power levels, whose values are shown in Fig. 14. The dashed line represents the overall acoustical-based reference level. It can be observed that no direct correlation is present between the number of initial sensors used in the improved process and the accuracy of the results in terms of overall sound power levels. Moreover, the differences between the overall vibration-based and the overall acoustical-based sound power levels change within the operational condition considered. In order to investigate the spectral similarity, the Γ index results are displayed in Fig. 15. The Figure illustrates that, by increasing the number of starting accelerometers, the similarity between the spectral components of the acoustical-based and vibration-based sound power levels is enhanced.

6. Insight into the radiation factor

As the literature review indicates, the frequency behavior knowledge of the radiation factor is limited to simple geometries. Therefore, it would be worthwhile to investigate the trend of this quantity for a real machine with varying torques and velocities. The following results have been obtained with the vibration-based procedure described in Sec. 2, considering twenty-seven accelerometers.

First, the influence of the rotational velocity will be discussed comparing the acoustical-based sound power levels (Fig. 16), the vibration-based sound power levels (Fig. 17) and the radiation efficiencies levels (Fig. 18) of tests with zero resistant torques. The acoustical-based sound power level increases with the increase of the velocity at frequencies higher than 400 Hz. At lower frequencies, the spectra show peaks at the

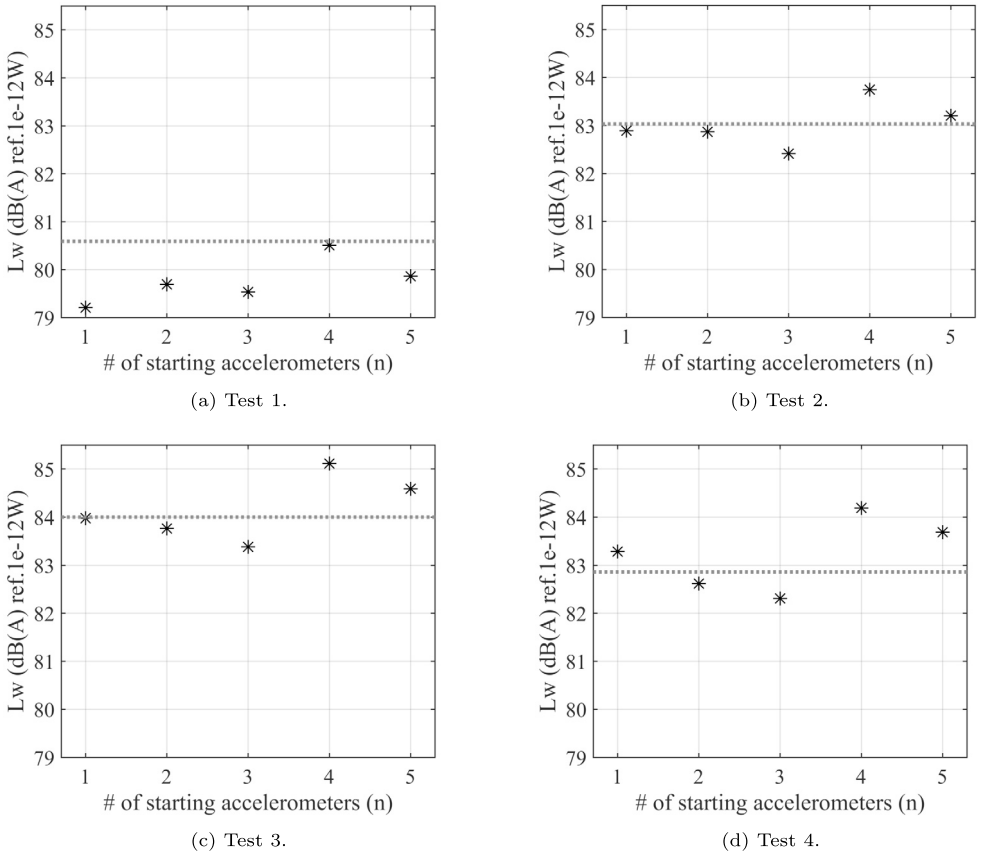

Fig. 14. Overall acoustical-based sound power level (:) and overall vibration-based sound power level (*) computed from the data of the k'' improved accelerometers.

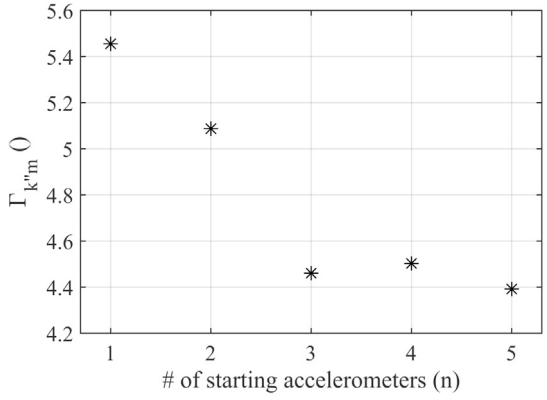

Fig. 15. Gamma index results computed from the data of the k'' improved accelerometers for different numbers of starting accelerometers.

power supply frequency of the electrical engine and its multiples. Similar assumptions may be formulated for the vibration-based sound power levels. The main differences were identified at low frequencies since the vibration-based sound power levels are more sensitive to the characteristic frequencies of the system. This leads to a better understanding of the behavior of the radiation factor at frequencies below 400 Hz, which exhibit the lowest values in the frequency range under consideration. Thus, the radiation efficiency level values of scenarios with different velocities show a good agreement: the rotational velocities do not affect the radiation factor behavior.

Then, the influence of different torques at the same power supply frequency of 70 Hz was investigated. The results of the acoustical-based sound power levels (Fig. 19), of the vibration-based sound power levels (Fig. 20) and of the radiation efficiency levels (Fig. 21) are quite similar considering the different torques, both in the octave bands and the overall levels. Regarding the tests with different velocities in Fig. 18a, lower differences were observed in the radiation efficiency levels at lower frequencies in Fig. 21a. This is due to the fact that the characteristic frequencies are the same as the velocity is the same. From these outcomes, it can be concluded that the resistant torque does not affect the radiation factor behavior.

Finally, the standard deviation of the obtained radiation efficiencies was shown in Fig. 22, considering the tests from 1 to 4 (summarized in Fig. 21) and the tests from 5 to 8 (summarized in Fig. 18). This quantity was obtained with the following formula:

$$\sigma_\sigma = \sqrt{\frac{1}{N_t - 1}\sum_{k_t=1}^{N_t}(\sigma_{j,k_t} - \overline{\sigma}_j)} \tag{9}$$

where N_t is the number of the considered test (equal to 8), which are 4 Nm, 8 Nm, 12 Nm and 18 Nm with power supply frequency of 70 Hz and zero resistant torque at 40 Hz, 60 Hz, 70 Hz and 80 Hz of power supply frequency. The mean values of the radiation efficiencies for each test and frequency band are represented by $\overline{\sigma}_j$. While σ_{j,k_t} denotes the octave band radiation efficiency for each of the considered tests k_t.
By analyzing Fig. 22, it was possible to understand how the radiation efficiency changes within the different octave bands, taking into account all the tests carried out. It was observed that the greatest discrepancies were observed in the 500 Hz octave band, while all other octave bands exhibited a deviation from the standard value of less than 0.7.

7. Concluding remarks

The vibration-based procedure to define the sound power level starting from the acceleration data has been described. The limit of the procedure is the requirement of several points of measurement. Since the

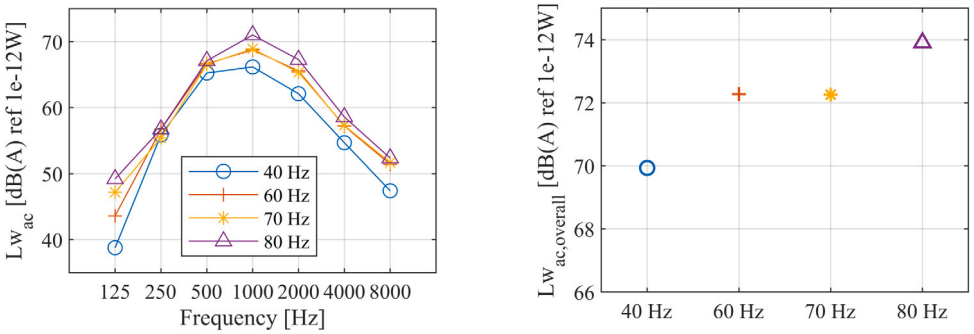

(a) Octave bands results. (b) Overall results.

Fig. 16. Acoustical-based sound power level. Zero resistant torque.

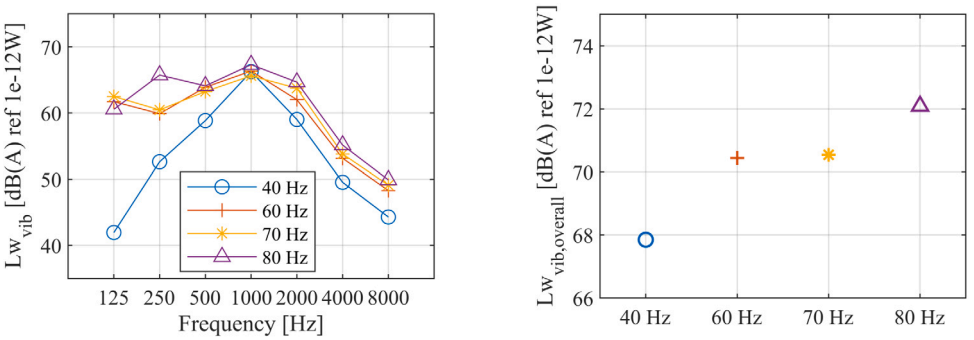

(a) Octave bands results. (b) Overall results.

Fig. 17. Vibration-based sound power level. Zero resistant torque.

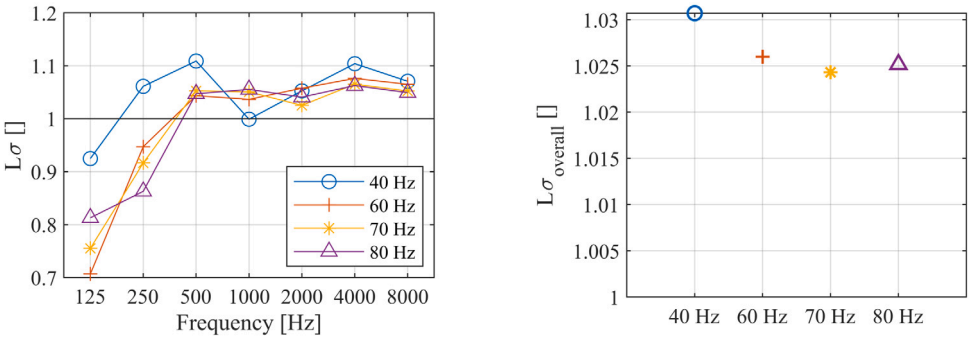

(a) Octave bands results. (b) Overall results.

Fig. 18. Radiation efficiency. Zero resistant torque.

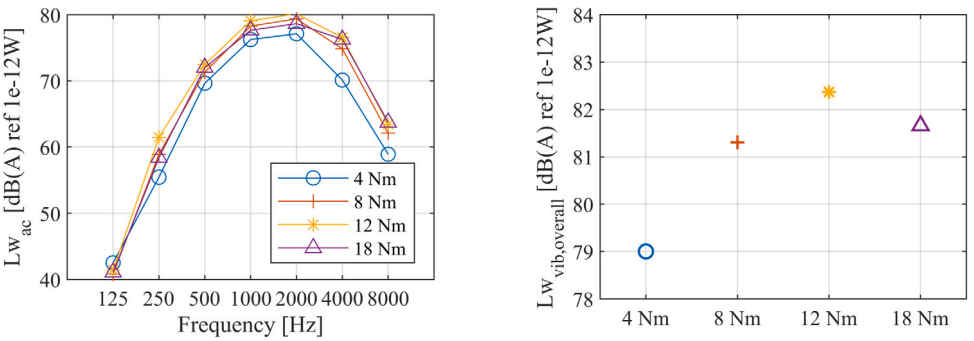

(a) Octave bands results. (b) Overall results.

Fig. 19. Acoustical-based sound power level. Power supply frequency of 70 Hz.

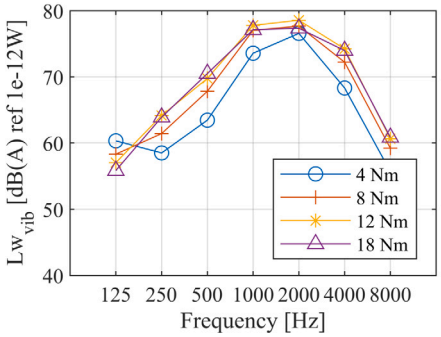

(a) Octave bands results. Power supply frequency of 70 Hz.

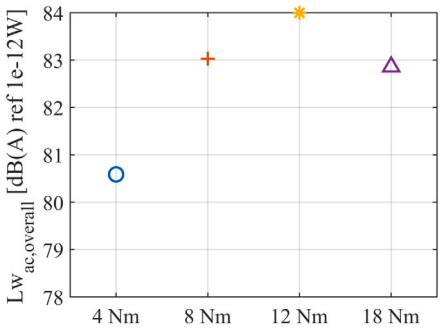

(b) Overall results.

Fig. 20. Vibration-based sound power level. Power supply frequency of 70 Hz.

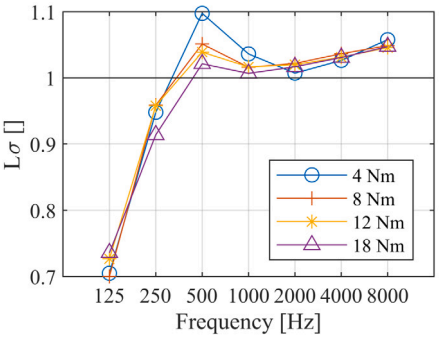

(a) Octave bands results.

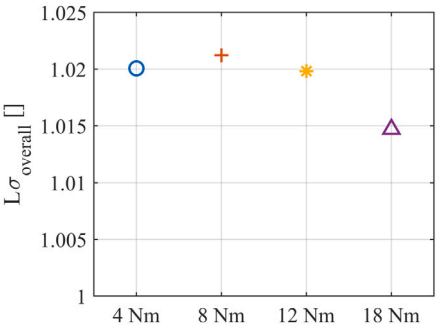

(b) Overall results.

Fig. 21. Radiation efficiency. Power supply frequency of 70 Hz.

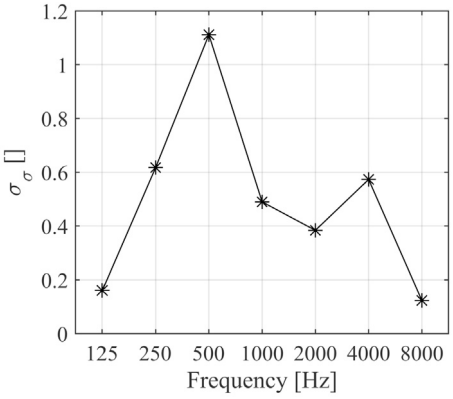

Fig. 22. Standard deviation of the radiation efficiency considering tests from 1 to 8.

employment of several accelerometers may be impractical and expensive, a new methodology to reduce the number of sensors was proposed to increase the ease of application of the vibration-based procedure. The aim was to find the position of n accelerometers that optimizes the results regarding the vibration-based sound power level, considering a radiation factor equal to one.

An experimental campaign validated the effectiveness of the procedure: the acoustical-based sound power level of the system under study was assessed from acoustical measurements (following the standard ISO 3746) and the vibration-based sound power level was computed from the acceleration signals acquired with twenty-seven sensors placed on the system surface. The correct number of accelerometers has been chosen following the Standard ISO 7849-2. Starting from these data, a novel approach for reducing the number of accelerometers was implemented and the following results were obtained.

- Singular operational condition with two accelerometers: the maximum difference between the vibration-based and the acoustical-based overall sound power level is 0.9 dB(A).
- Tests 1 to 4 with two accelerometers: the maximum difference between the vibration-based and the acoustical-based overall sound power level is 0.9 dB(A).
- Tests 1 to 4 with four accelerometers: the maximum difference between the vibration-based and the acoustical-based overall sound power level is 0.5 dB(A).

These outputs verify the proposed methodology.

Moreover, the influence of choosing a different number accelerometers in the improved procedure is investigated. By increasing the number of accelerometers, the number of combinations also increases, resulting in longer computational time. The overall sound power levels do not show a regular trend changing the accelerometers number, while the Γ index remains quite constant from three to five accelerometers as shown in Fig. 15. It may be concluded that the developed procedure, which reduces the number of sensors from the twenty-seven proposed by the Standard ISO 7849-2, is a reliable and effective instrument for determining the sound power level determination of a machine.

Therefore, the radiation efficiency was investigated to further understand the frequency trend and the impact of rotational velocity and applied torque. Within the increasing of the rotational velocities also the acoustical-based and vibration-based sound power levels increase. This consideration is true except for the low frequencies where the engine component appears and differs as the speed changes. As a consequence, the radiation factor frequency trend is similar between tests with different velocities. Likewise, an increase in the applied torque results in an increase of both the acoustical-based and vibration-based sound power levels: the radiation factor frequency trend is similar between tests with different torques.

CRediT authorship contribution statement

Giulia Cristofori: Writing – original draft, Validation, Methodology, Investigation, Data curation, Conceptualization. **Emiliano Mucchi:** Writing – review & editing, Project administration.

Declaration of competing interest

The authors declare that they have no known competing financial interests or personal relationships that could have appeared to influence the work reported in this paper.

Data availability

The data that has been used is confidential.

Acknowledgement

The authors thank the technicians of FAAC Industries for providing the experimental apparatus and for their assistance during the experimental campaign.

References

[1] ISO Central Secretary. Acoustics - determination of sound power levels and sound energy levels of noise sources using sound pressure - survey method using an enveloping measurement surface over a reflecting plane. Standard 3746, International Organization for Standardization; 2010.
[2] ISO Central Secretary. Acoustics — determination of sound power levels of noise sources using sound intensity – part 2: measurement by scanning.. Standard ISO 9614-2:1996, International Organization for Standardization; 1993.
[3] Fahy FJ. Sound and structural vibration: radiation, transmission and response. Elsevier; 2007.
[4] Hashimoto N. Measurement of sound radiation efficiency by the discrete calculation method. Appl Acoust 2001;62(4):429–46.
[5] Squicciarini G, Thompson D, Corradi R. The effect of different combinations of boundary conditions on the average radiation efficiency of rectangular plates. J Sound Vib 2014;333(17):3931–48.
[6] Wallace C. Radiation resistance of a rectangular panel. J Acoust Soc Am 1972;51(3B):946–52.
[7] Maidanik G. Response of ribbed panels to reverberant acoustic fields. J Acoust Soc Am 1962;34(6):809–26.
[8] Leppington FG, Broadbent EG, Heron K. The acoustic radiation efficiency of rectangular panels. Proc R Soc Lond Ser A, Math Phys Sci 1982;382(1783):245–71.
[9] Arenas JP, Crocker MJ. Sound radiation efficiency of a baffled rectangular plate excited by harmonic point forces using its surface resistance matrix. Int J Acoust Vib 2002;7(4):217–29.
[10] Putra A, Thompson D. Sound radiation from rectangular baffled and unbaffled plates. Appl Acoust 2010;71(12):1113–25.
[11] Arenas JP. Matrix method for estimating the sound power radiated from a vibrating plate for noise control engineering applications. Lat Am Appl Res 2009;39(4):345–52.
[12] Rayleigh JWSB. The theory of sound, vol. 2. Macmillan; 1896.
[13] Heckl M. Radiation from plane sound sources. Acta Acust Acust 1977;37(3):155–66.
[14] Conta S, Santoni A, Homb A. Benchmarking the vibration velocity-based measurement methods to determine the radiated sound power from floor elements under impact excitation. Appl Acoust 2020;169:107457.
[15] Santoni A, Fausti P, Schoenwald S, Tröbs H-M. Sound radiation efficiency measurements on cross-laminated timber plates. In: Inter-noise and noise-con congress and conference proceedings, vol. 253. Institute of Noise Control Engineering; 2016. p. 5979–89.
[16] Jacobson MF, Singh R, Oswald FB. Acoustic radiation efficiency models of a simple gearbox. National Aeronautics and Space Administration; 1996.
[17] Revel G, Rossi G. Sound power estimation by laser Doppler vibration measurement techniques. Shock Vib 1998;5(5–6):297–305.
[18] Yantek DS. Estimated sound power radiated by surfaces on a continuous miner tail section using vibration measurements; 2003.
[19] Abouel-Seoud SS, Mohamed ES, Abdel-Hamid AA, Abdallah AS. Analytical technique for predicting passenger car gearbox structure noise using vibration response analysis. Br J Appl Sci Technol 2013;3(4):860.
[20] Barelli L, Bidini G, Bonucci F, Moretti E. The radiation factor computation of energy systems by means of vibration and noise measurements: the case study of a cogenerative internal combustion engine. Appl Energy 2012;100:258–66.
[21] Gardonio P, Guernieri G, Turco E, Dal Bo L, Rinaldo R, Fusiello A. Reconstruction of the sound radiation field from flexural vibration measurements with multiple cameras. Mech Syst Signal Process 2023;195:110289.
[22] de Siqueira Nascimento ASB, Flesch RCC, Flesch CA. Data-driven soft sensor for the estimation of sound power levels of refrigeration compressors through vibration measurements. IEEE Trans Ind Electron 2019;67(8):7065–72.
[23] ISO Central Secretary. Acoustics — determination of airborne sound power levels emitted by machinery using vibration measurement – part 2: engineering method including determination of the adequate radiation factor. Standard ISO/TS 7849-2:2009, International Organization for Standardization; 2009.